www.sciencetranslationalmedicine.org/cgi/content/full/5/209/209ra152/DC1

Supplementary Materials for

Spherical Nucleic Acid Nanoparticle Conjugates as an RNAi-Based Therapy for Glioblastoma

Samuel A. Jensen, Emily S. Day, Caroline H. Ko, Lisa A. Hurley, Janina P. Luciano, Fotini M. Kouri, Timothy J. Merkel, Andrea J. Luthi, Pinal C. Patel, Joshua I. Cutler, Weston L. Daniel, Alexander W. Scott, Matthew W. Rotz, Thomas J. Meade, David A. Giljohann, Chad A. Mirkin,* Alexander H. Stegh*

*Corresponding author. E-mail: a-stegh@northwestern.edu (A.H.S.); chadnano@northwestern.edu (C.A.M.)

Published 30 October 2013, *Sci. Transl. Med.* **5**, 209ra152 (2013)
DOI: 10.1126/scitranslmed.3006839

This PDF file includes:

Other Supplementary Material for this manuscript includes the following:
(available at www.sciencetranslationalmedicine.org/cgi/content/full/5/209/209ra152/DC1)

Movie S1 (.mp4 format). 3D reconstruction of MR images after intracranial injection of Gd(III)-functionalized SNAs.

SUPPLEMENTARY METHODS

Repository of Molecular Brain Neoplasia Data (REMBRANDT)

REMBRANDT, a Web-based clinical genomics database, was used as a platform for data mining and analysis. Data were generated through the Glioma Molecular Diagnostic Initiative from 874 glioma specimens comprising ~566 gene expression arrays, 834 copy number arrays, and 13,472 clinical phenotype data points (*23*). Available at https://caintegrator.nci.nih.gov/rembrandt/.

RNA synthesis

RNA oligonucleotides were synthesized using TOM-RNA reagents (Glen Research) on a MerMade 6 system (Bioautomation) according to manufacturer-recommended cleavage and deprotection protocols. All oligonucleotides were purified using reverse-phase high performance liquid chromatography (RP-HPLC) on a Varian Microsorb C_{18} column (10 µm, 300 × 10 mm^2) with 0.1 M triethylammonium acetate (TEAA) at pH 7 with a 1%/min gradient of 100% CH_3CN at a flow rate of 3 ml/min, while monitoring the UV signal of the nucleic acids at 254 nm. The aqueous buffer was treated with 0.1% diethylpyrocarbonate (DEPC, Sigma) and autoclaved. After purification, the oligonucleotides were lyophilized and stored at -80°C until further use. siL12 sequences were designed to bind different regions of the *Bcl2L12* mRNA backbone, while the siCo sequence was a nonspecific control targeting *E. coli* β-galactosidase.

Gold nanoparticle functionalization

Citrate-stabilized gold nanoparticles (AuNPs, 13 ± 1 nm) were prepared using the Frens method (*43*). The particles were treated with DEPC (0.1% v/v) and autoclaved before being functionalized with siRNA duplexes as described previously (*9, 44*). Briefly, RNA duplexes terminated with propylthiol were hybridized and added to the RNase-free AuNPs, where they were allowed to chemisorb via the thiol-gold bond. To prevent dehybridization of the RNA duplex, the salt concentration of the AuNP solution was adjusted to 0.1 M with NaCl prior to duplex addition. Subsequently, the salt concentration was increased to 0.3 M NaCl over 12-24 h. RNA-functionalized particles were then treated with 30 μM of oligoethylene glycol-thiol (OEG-Thiol) or poly(ethylene glycol) (mPEG-Thiol) as an additional surface passivating ligand. Following synthesis, the SNAs were purified by three successive centrifugations steps, supernatant removal, and addition of phosphate buffered saline (PBS) at 4°C. Each siL12-2-SNA contained ~90 sense strands and ~38 antisense strands per 13 nm AuNP (table S1). For the generation of fluorochrome-labeled SNAs, Cy5 or Cy5.5 phosphoramidite (Glen Research) was manually coupled to the 5’ end of either siCo or siL12 sense strands prior to hybridization.

Gold nanoparticle characterization

Dynamic light scattering, zeta potential measurements, and an OliGreen assay were performed to confirm and quantify the presence of siRNA on AuNPs. In the OliGreen assay, 6.67 nM SNAs diluted in 8M urea were heated to 45°C for 20 min to dehybridize the antisense strands from the sense strands, which remain on the nanoparticle. The

sense-loaded AuNPs were pelleted by centrifugation, and the supernatant containing the antisense strands was collected and incubated with components of the Quant-iT OliGreen Assay (Invitrogen) for 5 min. Standards of known antisense RNA concentration were also incubated with OliGreen reagents to create a standard curve, and fluorescence was measured using a BioTek Synergy Microplate Reader with excitation/emission wavelengths of 485 nm/520 nm.

Synthesis of Gd(III)-SNAs

Gd(III)-SNAs were synthesized according to literature protocols (*15*) with slight modification. For this study, the azide and alkyne "click" functional groups of the DNA strands and Gd(III) complexes were reversed relative to previous studies. The alkyne-modified DNA was synthesized using standard phosphoramidite chemistry using "C8-Alkyne-dT-CE" phosphoramidite (Glen Research) within the sequence where alkyne functionality is desired. The azide-functionalized Gd(III) complexes used here are termed "pro-N3" complexes in (*42*). No other changes to the synthesis protocols were made.

siRNA transfection

Subconfluent glioma cells were transfected with siRNA oligonucleotides nonsense control (Dharmacon), siL12-1 (GGAGGACAGGCGGACCAGC), and siL12-2 (CUACAGAACAGCUCCACCA) at concentrations of 1 nM, 50 nM, and 100 nM using Oligofectamine or Lipofectamine 2000 (Invitrogen). The degree of *Bcl2L12* knockdown was determined 48 h after transfection.

Western blot analysis

For all Western blot analyses, proteins were separated by 4%–12% SDS-PAGE (Life Technologies), transferred to Hybond PVDF membranes (GE Healthcare), blocked with 5% milk in phosphate buffered saline with 0.1% Tween 20 (PBS/Tween) for 1 h, and incubated with the following antibodies: anti–cleaved caspase-3 (Cell Signaling), anti–cleaved caspase-7 (Cell Signaling), anti-Hsp70 (BD Pharmingen), anti-Bcl2L12 [anti-L12-1 antiserum (*16*)], anti-p21 (BD Pharmingen), anti-p53 (DO-1 clone, Santa Cruz), and anti-p-p53^{Ser15} (Cell Signaling). The blots were washed with PBS/Tween and developed with goat anti-rabbit or with goat anti-mouse IgG-HRP antibodies (Santa Cruz) in 5% milk PBS/Tween. After washing with PBS/Tween, the blots were developed with ECL Plus (GE Healthcare) following the manufacturer's protocol.

qRT-PCR

Total RNA isolated from cells using an RNeasy Kit (Quiagen) was transcribed into cDNA using M-MLV Reverse Transcriptase (Promega). qRT-PCR was performed using SYBR Green (ABI) with primers specific to *Bcl2L12* (CCATCGACAGAGAAGGAAGC and GCTACAGAACAGCTCCACCA), *p21* (ACACCACTGGAGGGTGACTT and CTGCCTCCTCCCAACTCAT) and *TATA-binding protein (TBP)* (GGCTGTTTAACTTCGCTTCC and CCTAGAGCATCTCCAGCACA) on a 7500 Real Time PCR System (Applied Biosystems). Results were analyzed and quantified using the ddCt method.

5’-RLM-RACE

5’-RLM-RACE was performed using the GeneRacer kit (Life Technologies) according to the manufacturer’s protocol with modifications. Briefly, U87MG cells were treated with 5 nM SNAs for 48 h, after which total RNA was harvested using the RNeasy kit (Qiagen). For the 5’-RACE reaction, 1.5-6.5 μg of total harvested RNA was ligated to 250ng GeneRacer oligo for 1 h at 37°C. The RNA was then phenol/cholorform extracted, precipitated with ethanol, and reverse transcribed with SuperScriptIII using a *Bcl2L12*-specific 3’ primer (L12RT, GTCCAATGGCAAGTTCAAGTC) for 50 min at 55°C followed by heat inactivation at 70°C for 15 min.

From this reaction, 2 μL was used for first round PCR using the Gene Racer 5’ primer and a *Bcl2L12*-specific 3’ primer (L12Rev, ACGGGTGAAACAGCCAGGATGCC), following the manufacturer’s cycling recommendations: 94°C for 2 min (1 cycle), 94°C for 30 sec, 72°C for 1 min (5 cycles), 94°C for 30 sec, 60°C for 30 sec, 72°C 1 min (25 cycles), and 72°C for 10 min (1 cycle). Another round of nested PCR was then performed using the GeneRacer 5’ nested primer and a *Bcl2L12*-specific nested primer (L12NRev, GTGAAGCTGTGCACGTGCT) with the following cycle parameters: 95°C for 2 min (1 cycle), 95°C for 30 sec, 60°C for 30 sec, 72°C for 10 min (40 cycles), and 72°C for 10 min. (1 cycle). PCR products were then separated on a 3% agarose gel, cut out, and sequenced to determine nucleotide sequence identity.

Scavenger receptor inhibition assay

U87MG cells were plated in 96-well plates (25,000 cells/well) 24 h prior to SNA addition. SNAs were added in the presence of polyinosinic acid (poly I), fucoidan, or methyl-β-cyclodextrin (Sigma) and incubated for 48 h. Cells were then trypsinized, counted using Countess (Invitrogen), and prepared for ICP-MS. SNA uptake into the cells was determined by dividing the number of gold nanoparticles per sample by the number of cells in the sample.

The impact of SR inhibition on in vitro BBB transcytosis was determined in a similar experiment as described above except the upper insert well was pre-treated with poly I (250 μg/mL) for 24 h prior to SNA delivery. Cy5.5-labeled SNAs (5 nM) were then added into the insert well, incubated for 24 h, and penetration across the huBMECs layer and into primary astrocytes was determined by fluorescence microscopy.

Evans blue dye passage across compromised BBB/BTB

Female CB17 SCID mice were orthotopically implanted with 1×10^5 U87 cells in 5 μL of volume in the same location as described for our in vivo distribution and efficacy studies. At days 7 and 21 following implantation, a 2% solution of Evans blue dye (EBD, Sigma) in 0.9% saline was injected intravenously via the tail vein at a dose of 2mL/kg into two mice. A control mouse without a tumor was also injected with EBD. Two hours following injection with EBD, mice were anesthetized with ketamine and xylazine at 100 mg/kg and 10 mg/kg, respectively. Under surgical plane anesthesia mice were sacrificed by decapitation and the brain extracted. Brains were washed briefly in DPBS for 15 seconds and placed in 4% paraformaldehyde at 4^oC.

SNA content in tissues

ICP-MS. All tissues were dried in an oven overnight, weighed, and digested with 3% HCl in nitric acid at 65°C overnight. Digested samples and standards of known gold concentration were diluted in 2% HCl and 2% HNO_3 with 5 ppb Indium as an internal standard, and analyzed on a ThermoFisher X Series II ICP-MS.

MRI and 3D movie reconstruction. The brain from xenografted mice injected i.c. with SNAs was excised and fixed in 4% paraformaldehyde for 24-48 h. Prior to MR imaging, it was rinsed and immersed in Fomblin. The sample was positioned in a 25-mm quadrature birdcage RF coil and imaged on a 9.4T Bruker Biospec MRI system (Bruker Biospin, Billerica, MA) with 12 cm diameter gradient insert. After localizer images were acquired, the brain was imaged using a T1-weighted 3D gradient echo sequence (FLASH) with repetition time (TR) of 15 ms, echo time (TE) of 6 ms, flip angle 30 degrees, 64 averages, matrix size 120 × 100 × 100, and field of view (FOV) 1.5 ×1.25 × 1.25 cm^3, resulting in 0.125 mm^3 isotropic resolution. Total scan time was 2 h 40 min. Images were acquired in a coronal or sagittal orientation and resliced using JIM software (Java Imaging Matrix) to an axial orientation. 3D reconstruction of the distribution of Gd(III)-SNA was performed by first segmenting the brain contour and the enhanced area of the 3D FLASH images using a semiautomated contouring method in JIM. The regions of interest were then used to create a stack of masked images for animation and rendering in Maya 2011 (Autodesk Inc) using Mental Ray (mental images GmbH).

LA-ICP-MS. Following the MR imaging, the brain was embedded in paraffin, and 10 µm coronal sections were obtained and stained with H&E. The laser ablation system

(UP213, New Wave Research) was coupled to an ICP-MS (X Series II, ThermoFisher Scientific) for spatially resolved elemental analysis of the brain sections. Operating parameters for the laser ablation system are as follows: 213 nm wavelength, 20 Hz repetition frequency, 80 µm spot diameter, 0.22 mJ laser power, 100 µm/s scan speed. The brain section was analyzed with sequential line scans spaced 80 µm apart in order to obtain 2D images of elemental distribution. The ablated material was transported from the sample chamber (SuperCell, New Wave Research) by helium (0.43 l/min) and argon (0.74 l/min) into the ICP-MS for analysis of ^{57}Fe, ^{66}Zn, ^{157}Gd, and ^{197}Au. The images were plotted using MATLAB R2007b (MathWorks Inc.).

Near-infrared fluorescence (NIRF) imaging. NIRF imaging studies were performed using a Caliper Life Sciences In Vivo Imaging System (IVIS) Spectrum to determine the extent of SNA accumulation in orthotopic glioma tumors following systemic delivery. U87MG (5×10^5 cells implanted) or huTNS tumors (2×10^5 cells implanted) were grown in the right cerebrum of CB17 SCID mice for 4 or 20 d, respectively. Isoflurane-anesthetized mice were imaged with the IVIS Spectrum using 675 nm/720 nm excitation/emission filters to establish baseline autofluorescence. The next day, mice received 100 µl Cy5.5-SNAs (1000 nM in U87 study and 750 nM in TNS study) or saline, and were imaged repeatedly over a two-day period. At the end of this timeframe, mice were humanely euthanized by carbon dioxide asphyxiation, and tissues were harvested for *ex vivo* NIRF imaging and quantification of gold by ICP-MS and silver staining. IVIS data was quantified by measuring radiant efficiency with Living Image software, and the signal in tumor-bearing brains was divided by the signal in non-tumor bearing brains to indicate relative SNA accumulation.

Silver staining. Brain samples were fixed in 10% formalin for 72 h then stored in 70% ethanol until they were paraffin-embedded and sectioned. Silver staining, which amplifies the size of nanoparticles via the deposition of silver on the gold, allows for visualization of gold presense by optical microscopy. Tissues were deparaffinized in xylene (10 min) and hydrated through a series of ethanol (100%, 90%, 70%, 50%; 3 min each) and water (3 min × 3 times). Silver enhancement was performed using the Silver Enhancement Kit for Light and Electron Microscopy (Ted Pella, Inc.). The samples were counterstained with Mayer's Hematoxylin, mounted with Vectamount AQ aqueous mounting medium, coverslipped, and dried.

Pharmacokinetics studies

Pharmacokinetic studies were performed in female CD1 mice (16-18 g). siL12-2-SNAs were administered in a single bolus injection via tail vein at a dose of 200 µg RNA/kg-body weight. Mice (n = 3 per time point) were sacrificed prior to administration and at 5, 10, 15, 30, and 45 min and 1, 2, 4, 8, 12, 16, 24, 48, and 72 h after administration. Blood was collected in a heparinized tube via cardiac puncture. In addition, liver, lungs, spleen, heart, kidneys, intestine and brain were obtained for mice sacrificed at 5 and 30 min, and at 4, 24, 48, and 72 h.

Gold content was analyzed via ICP-MS. For determination of pharmacokinetic parameters, the data were fit to a two-compartment model using non-linear regression analysis. This model assumes that particles are transported between the central and peripheral compartments with first-order kinetics and that particles are eliminated from the central compartment with first-order kinetics. The data were fit to eqn. S1, where Cp

is the concentration of the particles in blood; A and B are hybrid coefficients; α and β are rate constants for the distribution and elimination processes, respectively; and t is the time component.

$$Cp = Ae^{-\alpha t} + Be^{-\beta t} \qquad \text{(S1)}$$

Pharmacokinetic parameters were estimated using standard calculations. An initial data point at t=0 was included representing 100% of the injected dose in the blood. Calculated parameters include $\alpha t_{1/2}$ (half-life of particle distribution), $\beta t_{1/2}$ (half-life of particle elimination), VC (volume of the central compartment), Vd_{β} (volume of distribution during the elimination phase), AUC (area under the curve), and CLT (total body clearance).

Toxicology studies

Mouse cytokine study. Mice received 7 injections (total of ~10 mg/kg; RNA/body weight) as outlined in Fig. 4A. Blood samples were collected from mice on the day 21. Serum was separated and stored at -80°C until use. The serum samples were analysed using Milliplex MAP technology, a bead-based suspension array in which fluorescent-coded beads have cytokine capture antibodies on their surface to bind the proteins, following the manufacturer's recommended protocols (Millipore). Statistical significance was calculated by one-way ANOVA followed by Dunn's multiple comparison test.

Rat toxicity study. PBS or siL12-2-SNAs were administered to Sprague-Dawley rats (*n*=3) by i.v. injection as a single dose on day 1 (10 mg/kg; RNA/body weight). Animals were checked twice after injections (AM and PM) for mortality, abnormalities and sign of pain or distress. Cage-side observations were done before dosing at day 1 and

daily thereafter. Detailed observation was conducted on day 1 before dosing and on the scheduled sacrifice. Body weight was recorded before dosing, on day 1 (for 1 day toxicology study), or on day 14 (for 14 day toxicology study). Blood samples were collected for hematology and clinical chemistry. All blood tests were performed in Charles River Laboratories. Complete Blood Count included: white blood cells (WBC), red blood cells (RBC), hemoglobin, hematocrit, mean corpuscular volume (MCV), mean corpuscular hemoglobin (MCH), mean corpuscular hemoglobin concentration (MCHC), platelets (Plt), lymphocytes (Lymph), monocytes (Mono), eosinophils (EOS), and basophils (BASO). Blood chemistry included: aspartate aminotransferase (Ast), alanine aminotransferase (Alt), albumin, alkaline phosphatase (Alk), total bilirubin, creatinine, blood urea nitrogen (BUN), total protein, cholesterol, triglycerides, glucose, calcium, and inorganic phosphate (Phos). All animals were sacrificed and necropsied 14 d after SNA injection. All major organs were weighed and subjected to histopathological evaluation by H&E staining.

Immunohistochemistry

Brain samples were fixed in 10% formalin for 72 h then stored in 70% ethanol. Paraffin embedding, coronal sectioning, and H&E staining were performed. For immunohistochemistry, slides were placed in a 58-60°C oven overnight, de-waxed in xylene, and rehydrated. To retrieve antigen, slides were placed in citrate buffer [0.01 M citric acid (pH 6.0)] and pressure cooked at 125°C for 30 s. The temperature was gradually reduced to 90°C over 40 min. Slides were then cooled at room temperature for 20 min and placed in Dako Buffer. Dako Autostainer Plus or Leica Bond Max

Autostainer was used to stain tissue by the following method (with slight variations depending on antibody). Slides were blocked, treated with H_2O_2, incubated with primary antibodies [anti-CD31 (1:25, Abcam) or anti–cleaved caspase-3 (1:25, BioCare)] for 30 min, washed, incubated with secondary antibody for 15 min, washed and developed using DAB. For TUNEL staining, sections were deparaffinized, digested with Proteinase K, quenched for endogenous peroxide in H_2O_2, and then treated with Tdt Enzyme for 1 h at 37°C. Sections were then washed and treated with antidigoxigenin conjugate for 30 min at RT, washed, and developed with DAB.

SUPPLEMENTARY FIGURES

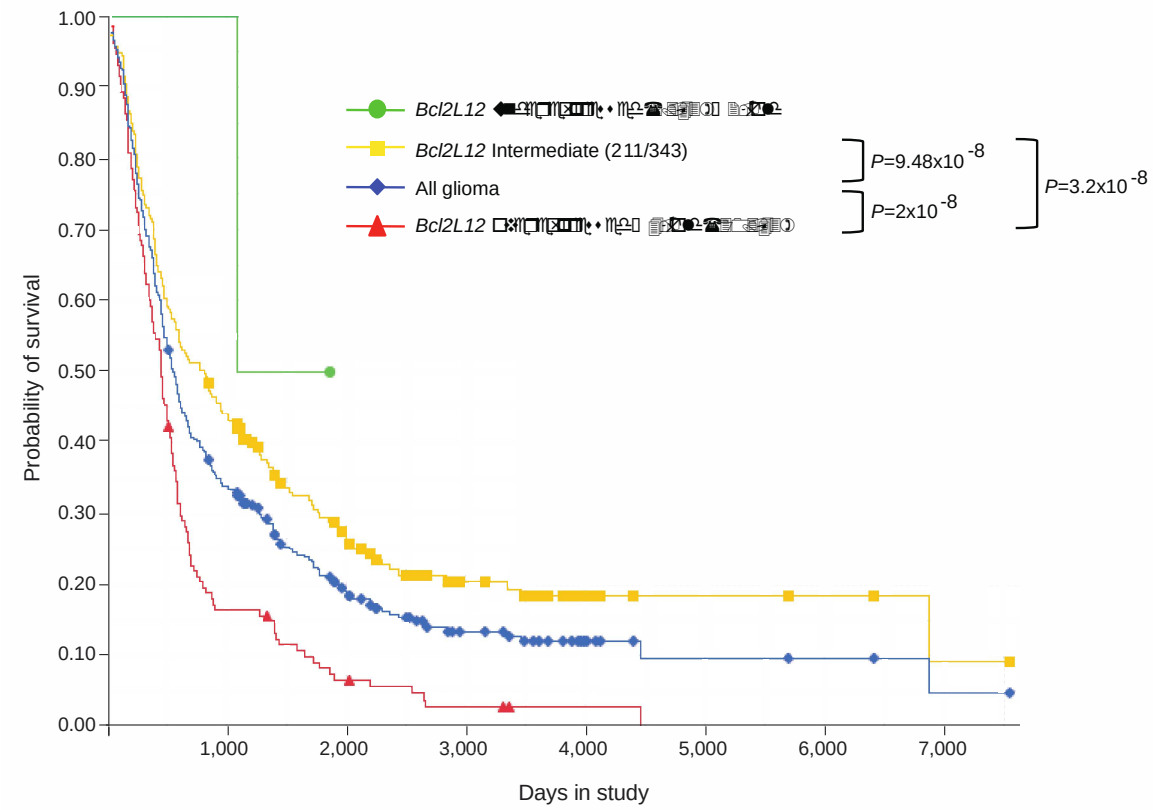

Fig. S1. *Bcl2L12* is a GBM oncogene. Survival analysis of 343 glioblastoma patients in REMBRANDT with differing levels of *Bcl2L12*. Log rank *P*-values calculated by REMBRANDT program using the Mantel-Haenszel procedure (*23*).

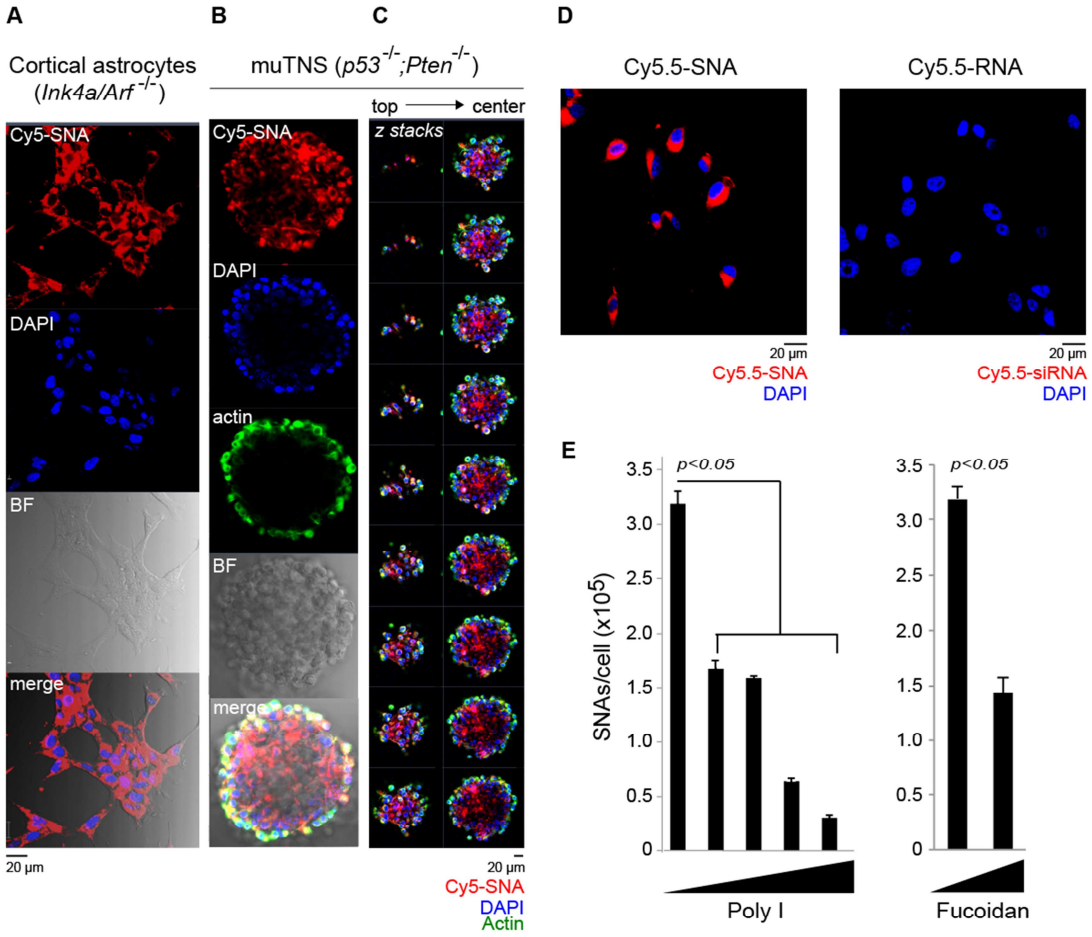

Fig. S2. SNA uptake into murine astrocytes and muTNS depends on scavenger receptors. (**A** to **C**) Cy5-labeled SNAs were taken up by transformed murine *Ink4a*/*Arf*-deficient cortical astrocytes (A) and muTNS derived from a GBM mouse model with CNS-specific deletion of *p53* and *PTEN* (genotype: *Pten*$^{-/-}$;*p53*$^{-/-}$) (B and C). Cells were co-labeled with fluorescent cytochalasin (green) and DAPI to visualize actin filaments and nuclei, respectively. (A and B) are representative confocal fluorescence images of murine astrocyte culture (n = 1) and muTNS cultures (n = 3), and (C) comprises various z sections of a muTNS. BF, bright field. (**D**) Fluorescence microscopy of U87MG cellular uptake of Cy5.5-siL12 oligonculeotides free in solution (siRNAs without a gold core) or Cy5.5-siL12-SNAs. (**E**) Cellular uptake of SNAs, as quantified by ICP-MS, by U87MG cells pre-incubated with increasing concentrations of polyinosinic acid (poly I; 0-250 µg/ml) or fucoidan (0-200 µg/ml) prior to administration of Cy5.5-SNAs. Data are means ± SD (n = 3 replicates). *P*-values calculated using two-tailed Student's *t*-test).

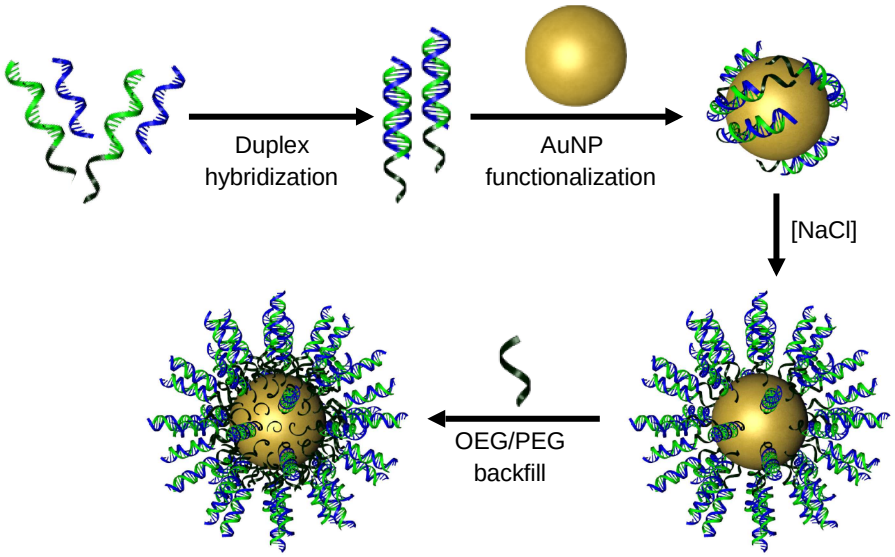

Fig. S3. Synthesis scheme for SNAs. RNA duplexes containing an ethylene glycol spacer and a propylthiol group were formed via hybridization, and incubated with RNase-free gold nanoparticles (AuNP). The salt concentration of the AuNP solution was adjusted with NaCl prior to duplex addition, followed by passivation of SNAs with oligoethylene glycol (OEG)-thiol or poly(ethylene glycol) (PEG)-thiol.

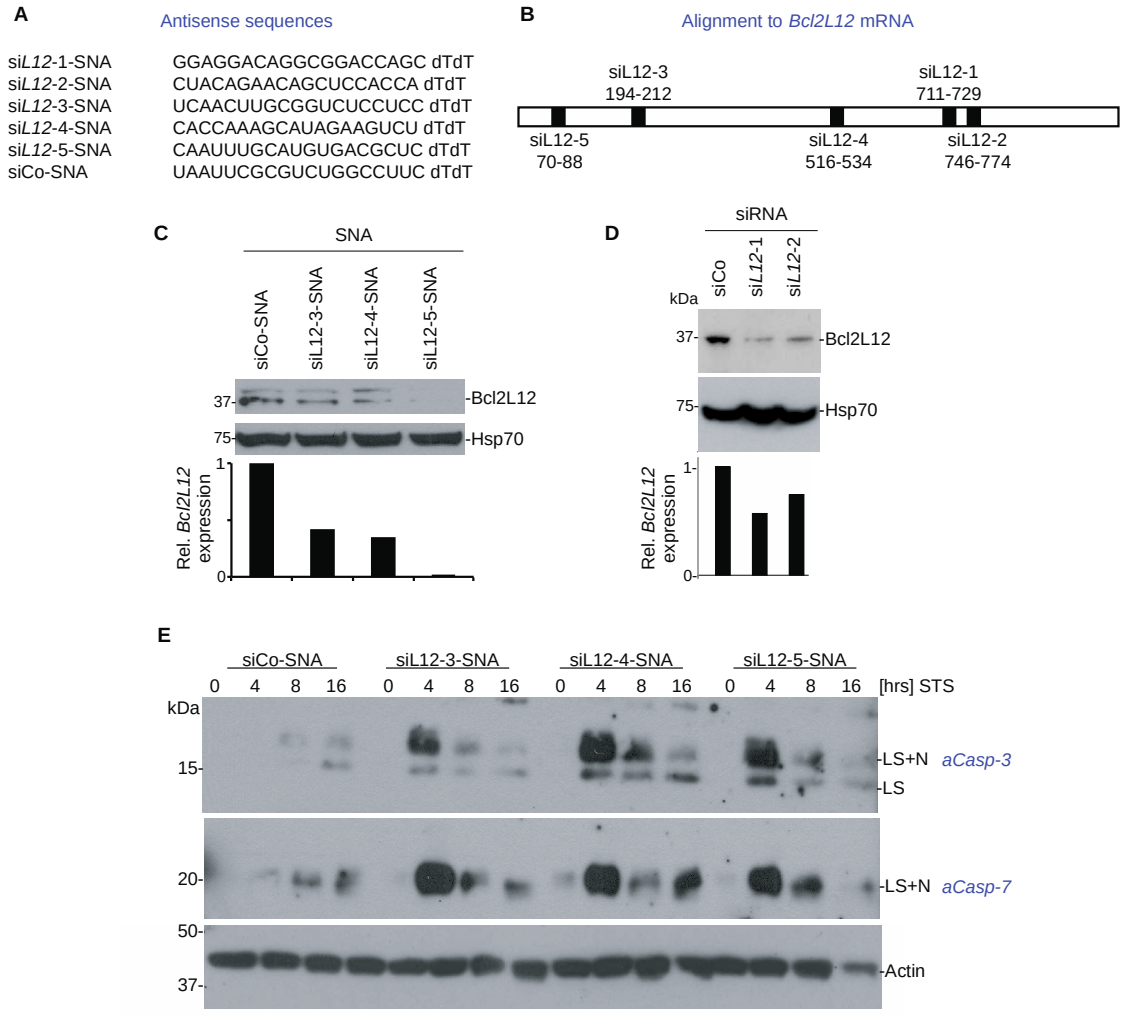

Fig. S4. **Evaluation of additional SNAs targeting *Bcl2L12*.** (**A**) Sequences of siRNAs for control- (siCo) and *Bcl2L12*-targeting (siL12-1 to -5) SNAs. (**B**) Binding sites of all five siL12-SNAs. **(C)** Impact of *Bcl2L12*-targeting SNAs (siL12-3 to -5) on Bcl2L12 protein levels in U87MG glioma cells relative to control (siCo-SNA) cultures, as assessed by Western blot. Migration positions of Bcl2L12 and Hsp70 (loading control) are shown. Graphs display densitometric analysis of Bcl2L12 normalized to Hsp70. (**D**) *Bcl2L12* knockdown upon lipoplex-mediated delivery of 100 nM free siRNA oligonucleotides as assessed by Western blot. Graphs display densitometric analysis of Bcl2L12 normalized to Hsp70. (**E**) Cellular sensitivity toward apoptosis in cells co-treated with siL12-SNAs or siCo-SNAs and STS. Shown is a Western blot for active caspase-3 and -7. LS, large subunit; LS+N, large subunit plus N-peptide. β-actin was the loading control.

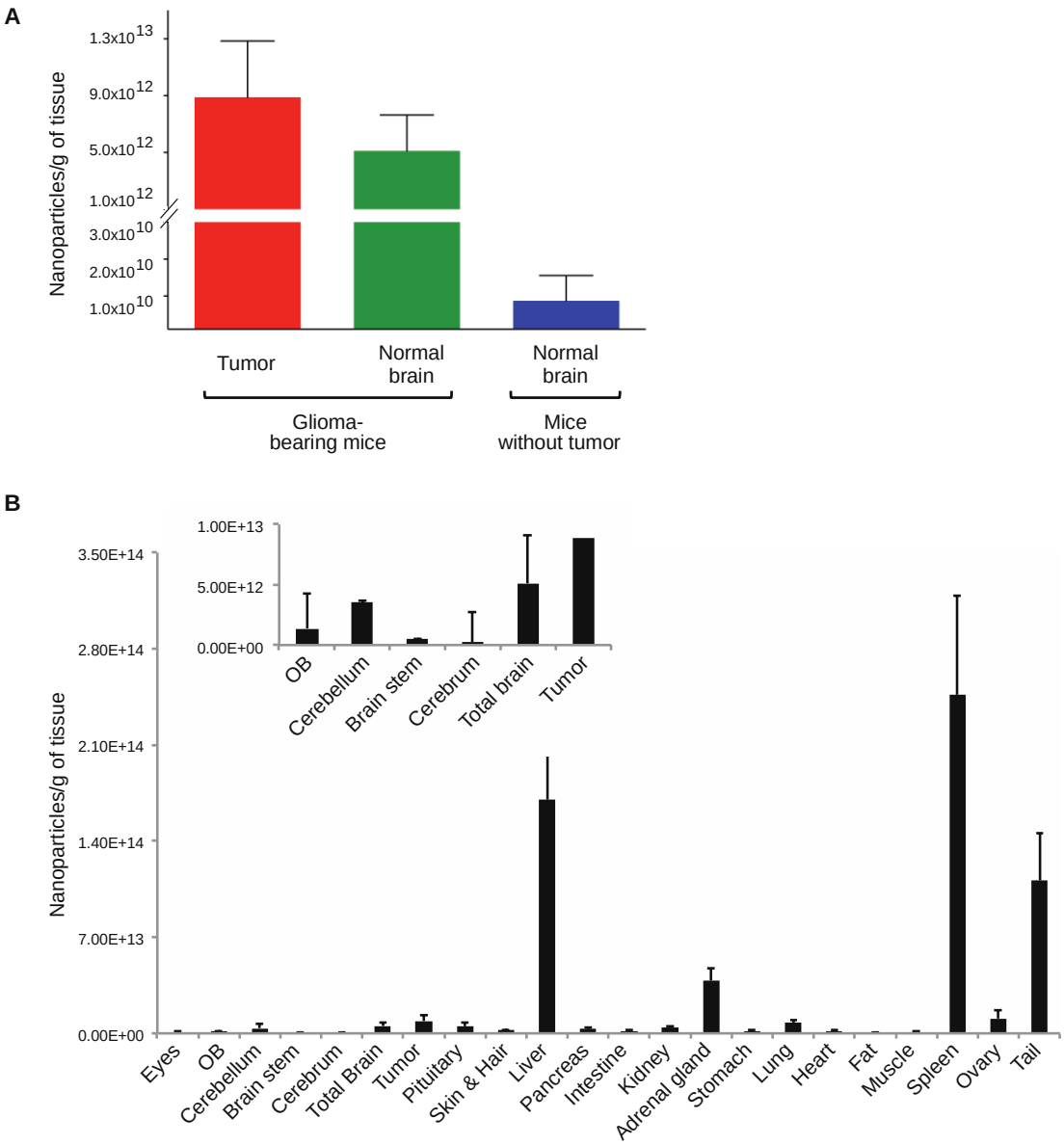

Fig. S5. **Biodistribution of SNAs in glioma-bearing mice after systemic administration.** (**A**) ICP-MS analysis of glioma and normal brain following intravenous (i.v.) injection of SNAs in glioma-bearing and normal mice. Mice were injected 5 times every other day, starting day 5 post-cell inoculation. Data are means ± SEM (n = 4 glioma-bearing mice, n = 3 mice without tumor). (**B**) SNA distribution in tumor, brain, and major organs upon systemic injection. Data are means ± SEM (n = 4 mice from one experiment). OB, olfactory bulb.

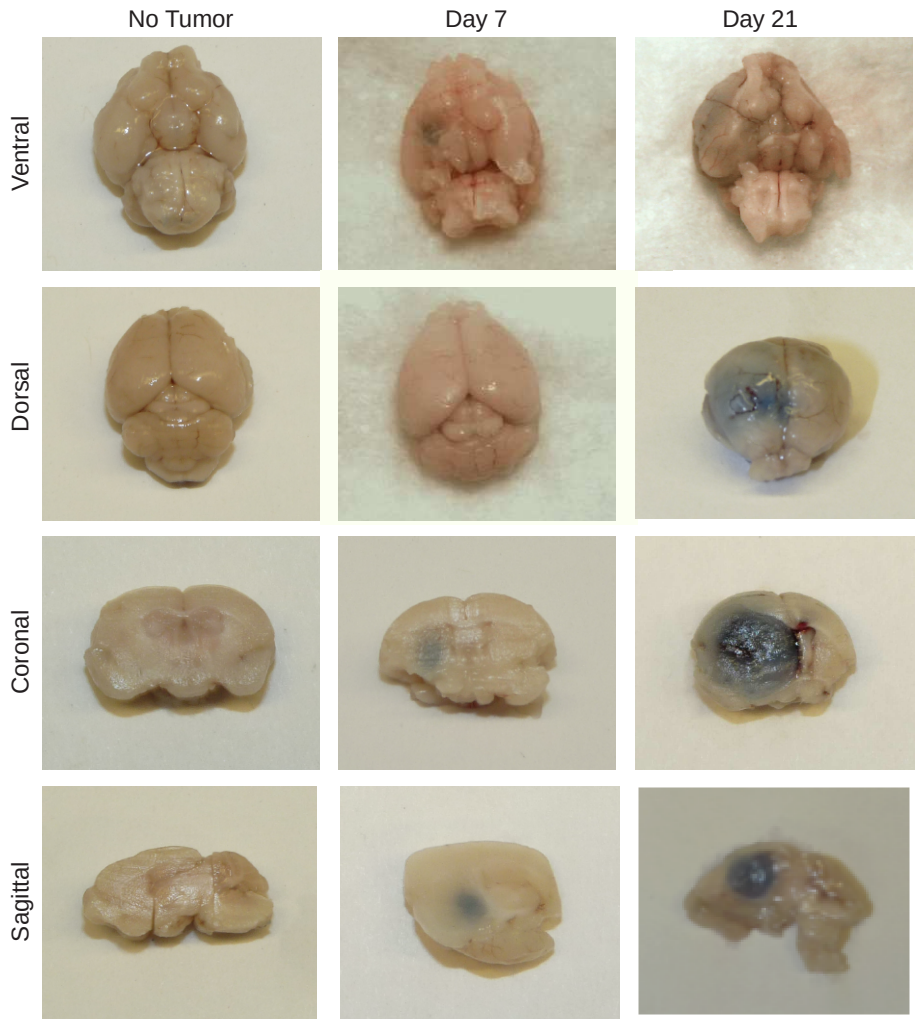

Fig. S6. **The BBB/BTB is compromised in tumor-bearing mouse brains.** Evans blue dye solution was intravenously administered to glioma-bearing mice (n = 3) at 7 and 21 days after U87MG cell inoculation, and allowed to circulate for 2 h. Shown are harvested brains at 7 and 21 days after tumor cell implantation as compared to a control brain (no tumor). Ventral and dorsal views of whole brain as well as coronal and sagittal sections are depicted.

A

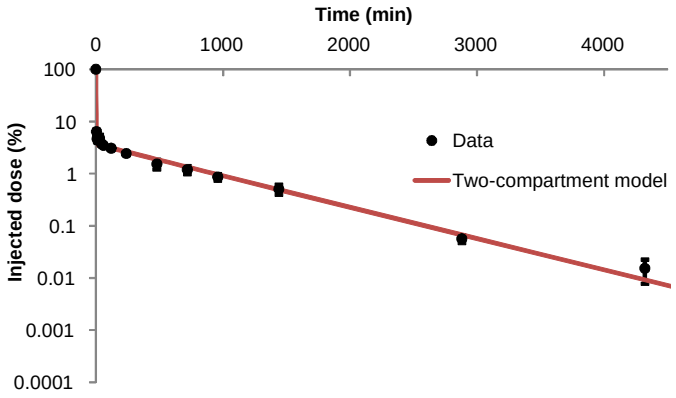

B

Two-compartment pharmacokinetics are described by
$[SNA] = Ae^{-\alpha t} + Be^{-\beta t}$

Hybrid coefficient	A	nmol/l	6.41
Hybrid coefficient	B	nmol/l	0.24
Rate constant for distribution phase	α	min^1	0.70
Rate constant for elimination phase	β	min^1	0.0014
Half-life of SNA distribution	$\alpha t_{1/2}$	min	0.98
Half-life of SNA elimination	$\beta t_{1/2}$	min	500.4
Volume of the central compartment	V_C	l/kg	0.070
Volume of distribution during elimination phase	Vd_β	l/kg	1.74
Area under the curve	AUC	nmol*min/l	184
Total body clearance	CL_T	ml/min/kg	2.54

Fig. S7. Pharmacokinetics of SNAs. The distribution and clearance of SNAs were studied by measuring gold content in blood and other tissues by ICP-MS. (**A**) Data were fit to a two-compartment model using non-linear regression analysis, suggesting that transport between the central and peripheral compartments and elimination of SNA conjugates follow first-order kinetics. Each data point displays the average gold content in blood for *n* = 3 mice per time point. (**B**) Pharmacokinetic parameters of SNA distribution and elimination, determined from the two-compartment pK analysis described in (A).

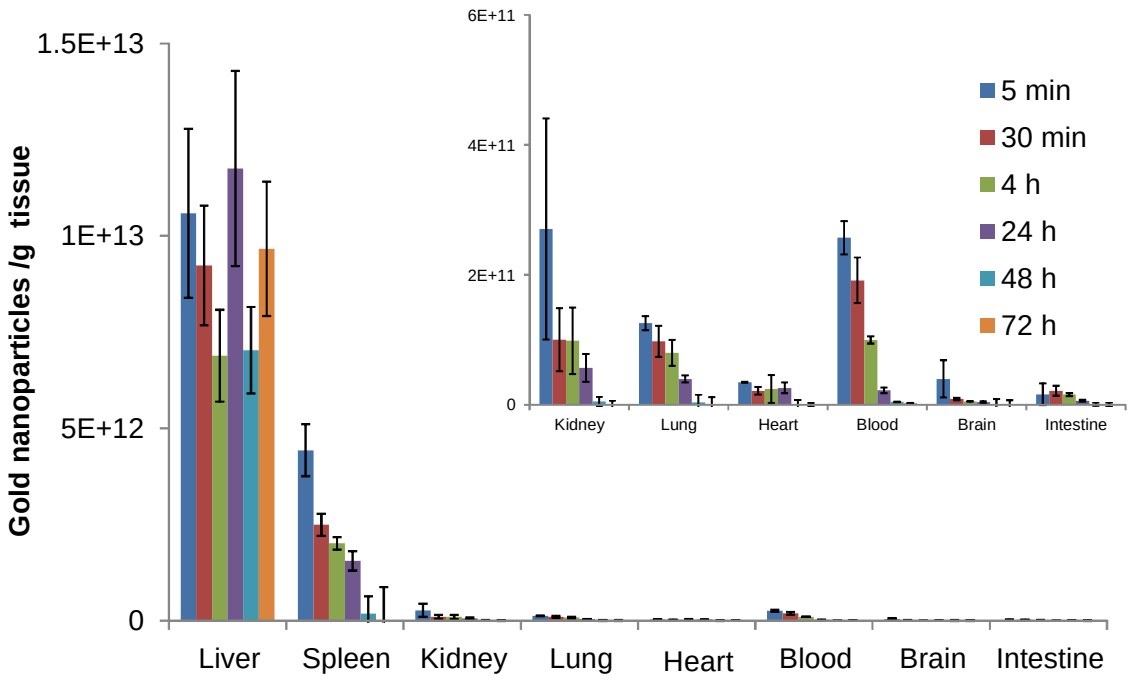

Fig. S8. Biodistribution of SNAs in tumor-free mice. The distribution of SNAs was studied in non-tumor-bearing mice by measuring gold content in tissues by ICP-MS following a single bolus injection of SNAs (n = 3 mice per time point).

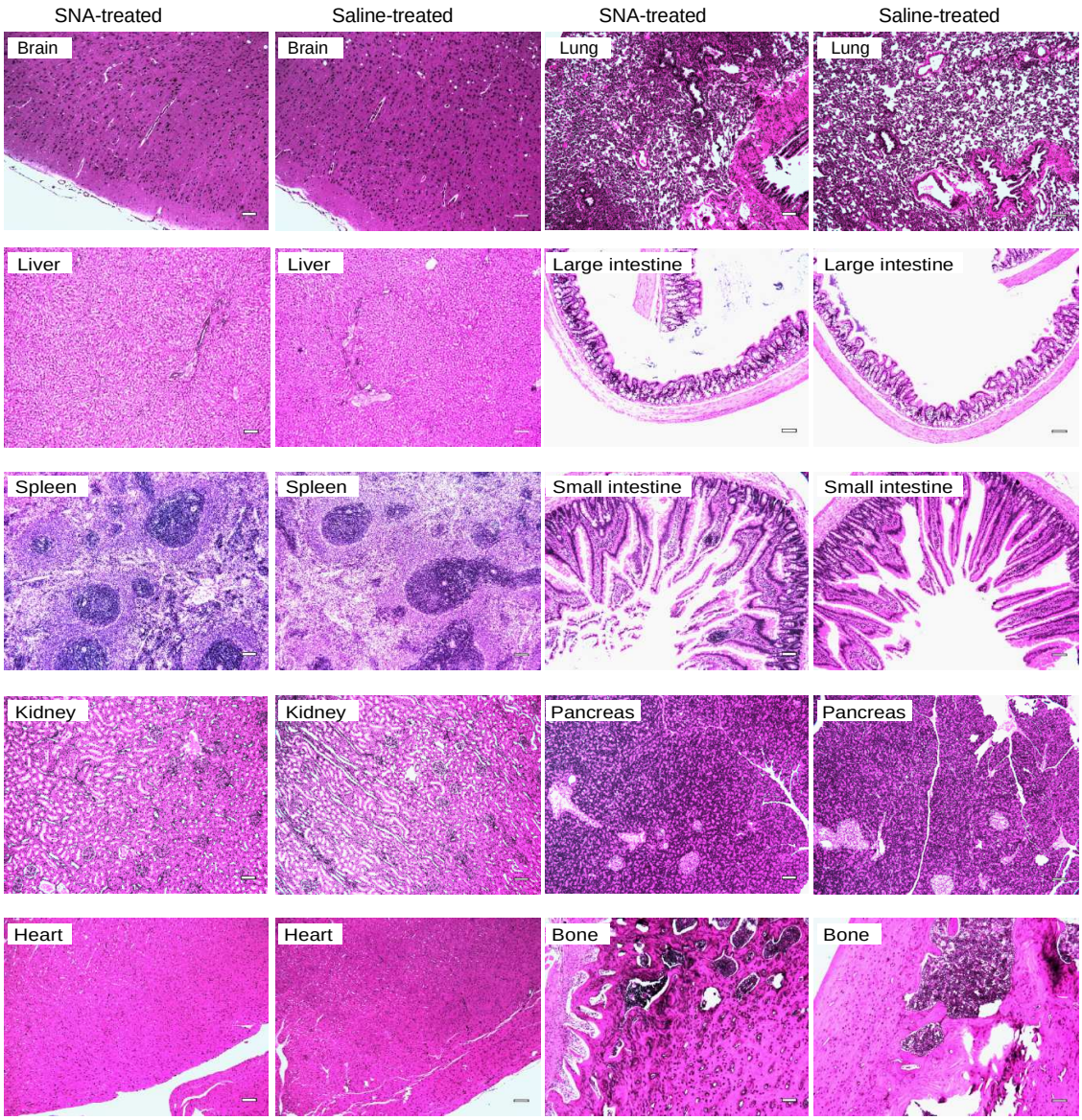

Fig. S9. Histological evaluation of siL12-2-SNAs in major tissues. Sprague-Dawley rats (n = 6 per group) injected intravenously with siL12-2-SNAs (10 mg/kg) or equivalent volume of saline were evaluated 14 days after treatment. Representative H&E-stained brain, liver, spleen, kidney, heart, lung, large intestine, small intestine, pancreas, and bone are shown. Scale bars, 500 μm.

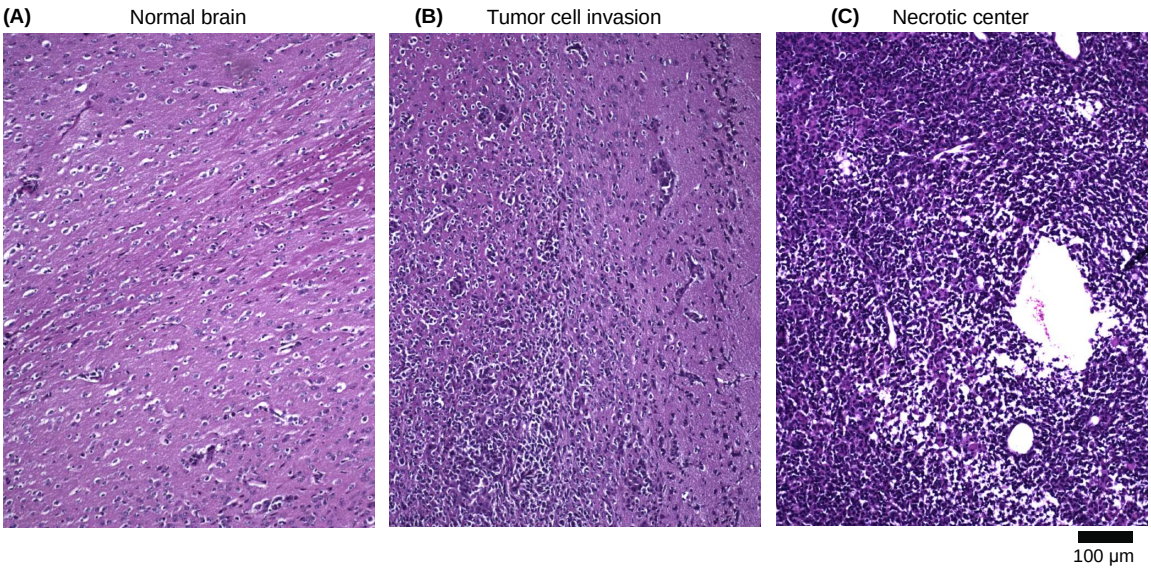

Fig. S10. Histological analysis of huTNS-derived mouse tumors. Representative H&E stained tissues from mouse tumors (n = 3) resulting from inoculation of huTNS cells. (**A**) Normal brain. (**B**) Hypercellular tumor tissue with extensive and diffuse invasion into surrounding normal brain. (**C**) Necrotic tumor core.

SUPPLEMENTARY TABLES

Table S1. Characterization of SNAs. Hydrodynamic diameter of gold nanoparticles increased and zeta potential decreased upon addition of siRNA and backfill molecules, indicating successful surface conjugation. A fluorescence-based Oligreen assay was used to quantify the number of antisense strands present per L12-2-SNA. AuNP, gold nanoparticle. Data are means ± SD (n = 6 replicates from one test for zeta potential, hydrodynamic diameter, and PDI; three independent tests for antisense loading).

	Zeta potential (mV)	Hydrodynamic diameter (nm)	Poly dispersity index (PDI)	Antisense loading (strands per AuNP)
Bare AuNP	-24.6 ± 2.7	19.0 ± 0.4	0.10 ± 0.02	NA
siCo-SNA	-32.5 ± 0.6	30.5 ± 0.7	0.18 ± 0.02	25.4 ± 1.9
siL12-2-SNA	-33.5 ± 1.3	33.6 ± 0.2	0.14 ± 0.02	37.8 ± 5.3

Table S2. Evaluation of serum cytokines in mice. Data are means +/- SD of *n*=3-5 mice injected with equal volumes of saline, siCo-SNAs, or siL12-2-SNAs. Saline or SNAs were injected every other day from days 7 to 16 post tumor inoculation, and serum samples were collected on day 21. All values were within normal range and no significant difference was observed between the groups in this single study. Statistical significance was calculated by one-way ANOVA followed by Dunn's multiple comparison test. G-CSF = granulocyte colony-stimulating factor; GM-CSF = granulocyte-macrophage CSF; IFN = interferon; IL = interleukin; IP = IFN□-induced protein; LIX = lipopolysaccharide induced C-X-C motif chemokine; KC = keratinocyte chemoattractant, also known as C-X-C motif chemokine ligand 1 (CXCL1); MCP = monocyte chemoattractant protein; MIP = macrophage inflammatory protein; M-CSF = macrophage CSF; MIG = monokine induced by IFN□; TNF = tumor necrosis factor.

Cytokine	Saline *n* = 3			siCo-SNA *n* = 5			siL12-2-SNA *n* = 5		
G-CSF	155.3	±	36.9	372.4	±	124.5	228.7	±	65.1
Eotaxin	1145.3	±	108.4	1068.2	±	200.7	726.3	±	140.8
GM-CSF	52.6	±	4.6	55.1	±	12.9	36.6	±	8.1
IFN□	11.3	±	2.4	10.0	±	1.9	5.9	±	1.3
IL-1α	427.3	±	132.7	244.7	±	48.2	367.7	±	107.0
IL-2	21.5	±	6.7	13.7	±	3.5	15.2	±	1.0
IL-5	22.3	±	7.1	30.4	±	15.5	17.0	±	5.5
IL-6	8.7	±	1.3	12.4	±	3.0	12.2	±	2.9
IL-7	7.9	±	1.8	6.0	±	1.3	5.2	±	0.8
IL-10	12.5	±	0.7	9.4	±	2.8	6.8	±	1.0
IL-12 (p40)	35.5	±	1.6	30.7	±	4.4	22.5	±	4.2
IL-12 (p70)	18.9	±	2.9	20.4	±	3.4	15.4	±	4.2
IL-13	209.3	±	34.6	209.6	±	33.3	145.5	±	33.9
LIX	14225.3	±	258.9	14221.4	±	575.0	13593.7	±	293.7
IL-15	71.6	±	7.5	57.1	±	13.3	42.0	±	15.0
IL-17	5.6	±	1.1	4.6	±	0.6	4.2	±	0.7
IP-10	158.0	±	9.3	290.2	±	76.4	193.0	±	49.2
KC	266.0	±	114.9	320.8	±	71.8	226.3	±	13.0
MCP-1	60.0	±	1.8	63.0	±	10.1	44.3	±	8.2
MIP-1α	99.4	±	12.8	94.2	±	6.7	75.9	±	6.4
MIP-1β	96.0	±	8.0	104.3	±	8.6	82.3	±	13.8
M-CSF	35.4	±	3.7	35.5	±	5.2	22.9	±	5.9
MIP-2	121.2	±	15.0	85.5	±	10.3	73.2	±	14.2
MIG	59.0	±	42.5	72.8	±	37.6	29.3	±	11.5
TNFα	10.3	±	1.1	9.5	±	1.8	7.5	±	1.8

Table S3. Body weight and blood chemistry after systemic SNA administration to Sprague-Dawley rats. Data are means +/- SD for female (*n*=3) and male (*n*=3) rats injected intravenously with siL12-2-SNAs (10 mg/kg) or an equal volume of PBS. Normal ranges for these values were provided by Charles Rivers Labs for CD rats. Measured parameters include aspartate aminotransferase (Ast), alanine aminotransferase (Alt), alkaline phosphatase (Alk), inorganic phosphate (Phos), blood urea nitrogen (Bun), white blood cells (WBC), neutrophils (Neut), lymphosites (Lymph), monocytes (Mono), eosinophils (Eos), basophils (Baso), large unstained cells (LUC), red blood cells (RBC), mean corpuscular volume (MCV), mean corpuscular hemoglobin (MCH), mean corpuscular hemoglobin concentration (MCHC), red cell distribution width (RDW), platelets (PLT), and mean platelets volume (MPV). (Other parameters are spelled out in the table.)

	Female (PBS)	Female (SNAs)	Female (PBS)	Female (SNAs)	Normal value range (female)	Male (PBS)	Male (SNAs)	Male (PBS)	Male (SNAs)	Normal value range (male)
	24 hours		14 days			24 hours		14 days		
Initial weight (g)	214.2 ± 0.7	228.0 ± 7.6	212.7 ± 2.2	225.6 ± 3.0		258.5 ± 8.8	253.7 ± 4.2	254.9 ± 3.3	267.7 ± 4.6	
Terminal weight (g)	218.6 ± 1.1	233.6 ± 7.2	260.3 ± 6.9	273.6 ± 7.8		266.4 ± 11.1	262.3 ± 3.2	372.3 ± 3.5	391.0 ± 11.2	
Cholesterol (mg/dl)	71 ± 2.3	75.7 ± 6.3	72.0 ± 4.5	76.3 ± 1.2	60 - 152	61.3 ± 4.2	65.3 ± 0.3	72.3 ± 3.5	70.7 ± 9.3	64 – 158
Triglycerides (mg/dl)	71.0 ± 4.6	60.7 ± 5.2	87.7 ± 35.2	98.0 ± 22.9	41 - 330	77.0 ± 17.0	79.7 ± 11.8	95.7 ± 5.3	128.3 ± 20.4	48 – 418
Ast (U/l)	68 ± 11.4	81 ± 6.7	99 ± 4.9	96 ± 11.0	52 - 310	71 ± 5.4	155 ± 39.7	68.3 ± 2.7	87.0 ± 7.1	64 – 386
Alt (U/l)	43 ± 4.8	42 ± 0.7	50 ± 5.6	47 ± 4.8	32 - 93	42 ± 3.3	54 ± 4.6	42 ± 1.2	41 ± 1.5	37 – 178
Alk (U/l)	212 ± 44.9	151 ± 17.8	221 ± 43.5	161 ± 27.1	61 - 359	351 ± 19.9	499 ± 32.3	245 ± 15.1	329 ± 51.2	134 – 588
Glucose (mg/dl)	191 ± 10.8	202 ± 7.2	205 ± 12.0	187 ± 23.6	122 - 456	162 ± 3.8	214 ± 6.6	216 ± 11.2	192 ± 3.6	110 – 456
Calcium (mg/dl)	10.3 ± 0.4	10.9 ± 0.09	10.8 ± 0.2	11.1 ± 0.1	10.4 - 14.2	9.9 ± 0.3	10.9 ± 0.07	10.8 ± 0.03	11.1 ± 0.2	10.3 - 14.3
Phos (mg/dl)	8.5 ± 0.2	9.0 ± 0.1	7.7 ± 0.5	7.4 ± 0.2	7.1 - 14.6	7.7 ± 0.5	10.0 ± 0.4	8.0 ± 0.3	9.1 ± 0.3	7.9 - 16.6
Total bilirubin (mg/dl)	0.1 ± 0.0	0.1 ± 0.0	0.1 ± 0.03	0.1 ± 0.0	0.1 -0.3	0.1 ± 0.0	0.1 ± 0.03	0.1 ± 0.0	0.1 ± 0.0	0.1 - 0.4
Creatinine (mg/dl)	0.3 ± 0.03	0.3 ± 0.0	0.3 ± 0.0	0.4 ± 0.03	0.3 - 0.6	0.2 ± 0.0	0.3 ± 0.03	0.3 ± 0.0	0.3 ± 0.0	0.3 - 0.7
Bun (mg/dl)	13 ± 1	12 ± 1	16 ± 1	14 ± 1	7 - 22	10.3 ± 0.7	12.7 ± 0.7	13.7 ± 1.2	14.7 ± 0.9	7 -23
Total protein (g/dl)	5.2 ± 0.3	5.9 ± 0.2	5.6 ± 0.1	5.8 ± 0.2	6.2 - 8.5	4.6 ± 0.1	5.2 ± 0.06	5.5 ± 0.1	5.6 ± 0.09	6.0 - 8.2
Albumin (g/dl)	3.1 ± 0.1	3.4 ± 0.1	3.7 ± 0.1	3.7 ± 0.1	3.3 - 4.7	2.6 ± 0.03	2.9 ± 0.03	3.4 ± 0.0	3.4 ± 0.07	3.2 - 4.4
Sodium (mEq/l)	130.6 ± 5.5	137.6 ± 0.9	138.3 ± 0.8	139.1 ± 0.5	137.7 - 169.7	125.6 ± 4.0	139.5 ± 0.8	140.2 ± 0.6	140.2 ± 0.4	138.3 - 171.3
Potassium (mEq/l)	4.26 ± 0.40	4.26 ± 0.21	4.90 ± 0.25	4.50 ± 0.23	5.58 - 10.73	4.51 ± 0.05	4.92 ± 0.36	4.73 ± 0.11	4.87 ± 0.13	5.98 - 11.90
Chloride (mEq/l)	91.5 ± 3.7	98.2 ± 0.7	100.4 ± 1.1	100.7 ± 0.9	96.7 - 119.7	89.4 ± 2.4	100.3 ± 0.2	99.5 ± 0.3	99.8 ± 0.2	95.8 - 120.3
WBC (x10^3 cells/µl)	6.09 ± 0.44	8.26 ± 0.44	10.27 ± 2.03	8.30 ± 0.95	2.40 - 17.68	8.51 ± 1.06	6.85 ± 0.93	10.97 ± 1.51	9.72 ± 1.45	4.01 - 18.02
#Neut (x10^3 cells/µl)	1.16 ± 0.29	1.72 ± 0.08	2.03 ± 0.46	1.26 ± 0.38	0.68 - 5.85	1.73 ± 0.22	1.29 ± 0.03	1.72 ± 0.20	1.98 ± 0.33	0.98 - 6.73
#Lymph (x10^3 cells/µl)	4.47 ± 0.68	5.87 ± 0.44	7.60 ± 1.71	6.64 ± 0.55	1.49 - 11.54	6.18 ± 1.01	5.09 ± 0.85	8.73 ± 1.32	7.22 ± 1.13	2.21 - 12.00
#Mono (x10^3 cells/µl)	0.14 ± 0.04	0.27 ± 0.01	0.21 ± 0.04	0.16 ± 0.03	0.11 - 1.21	0.21 ± 0.05	0.16 ± 0.05	0.24 ± 0.03	0.22 ± 0.04	0.18 - 1.43
#Eos (x10^3 cells/µl)	0.23 ± 0.13	0.24 ± 0.11	0.28 ± 0.04	0.09 ± 0.01	0.01 - 0.48	0.26 ± 0.08	0.21 ± 0.06	0.09 ± 0.01	0.12 ± 0.0	0.01 - 0.50
#Baso (x10^3 cells/µl)	0.01 ± 0.0	0.02 ± 0.01	0.04 ± 0.01	0.02 ± 0.01	0.00 - 0.16	0.02 ± 0.0	0.02 ± 0.0	0.04 ± 0.01	0.04 ± 0.01	0.00 - 0.17

#LUC (x10^3 cells/µl)	0.07 ± 0.01	0.14 ± 0.02	0.1 ± 0.02	0.12 ± 0.03		0.1 ± 0.01	0.09 ± 0.0	0.2 ± 0.04	0.13 ± 0.01	
Neut (%)	19.4 ± 5.0	21.0 ± 1.6	20.3 ± 3.0	14.5 ± 3.3	13.75 - 54.79	20.7 ± 3.4	19.6 ± 2.6	15.9 ± 1.6	20.4 ± 2.1	16.01 - 53.86
Lymph (%)	72.9 ± 7.5	70.9 ± 1.0	73.0 ± 3.9	80.8 ± 3.7	37.04 - 81.16	72.0 ± 5.0	73.4 ± 2.8	79.3 ± 1.6	74.2 ± 2.2	37.76 - 78.86
Mono (%)	2.4 ± 0.7	3.4 ± 0.3	2.1 ± 0.2	1.9 ± 0.2	2.8 - 11.0	2.4 ± 0.3	2.3 ± 0.6	2.2 ± 0.2	2.2 ± 0.03	3.13 - 10. 74
Eos (%)	3.9 ± 2.0	2.7 ± 1.1	3.3 ± 1.3	1.1 ± 0.09	0.16 - 4.7 7	3.2 ± 1.3	3.1 ± 0.7	0.8 ± 0.09	1.3 ± 0.2	0.14 - 4 .31
Baso (%)	0.2 ± 0.0	0.27 ± 0.03	0.37 ± 0.09	0.3 ± 0.06	0.00 - 1.56	0.3 ± 0.03	0.2 ± 0.03	0.3 ± 0.03	0.5 ± 0.03	0 .00 - 1.67
Luc (%)	1.2 ± 0.2	1.7 ± 0.4	1.0 ± 0.09	1.4 ± 0.2		1.4 ± 0.2	1.4 ± 0.2	1.4 ± 0.2	1.4 ± 0.09	
RBC (x10^6 cells/µl)	6.89 ± 0.41	6.43 ± 0.15	7.12 ± 0.07	7.15 ± 0.30	5.5 3 - 9.83	6.29 ± 0.14	6.26 ± 0.17	7.26 ± 0.13	6.98 ± 0.08	5.84 - 9.96
Hemoglobin (g/dl)	14.2 ± 0.8	13.7 ± 0.1	14.2 ± 0.03	14.4 ± 0.3	12.6 - 22.2	13.6 ± 0.17	13.4 ± 0.15	14.5 ± 0.03	14.0 ± 0. 18	13.1 - 23.1
Hematocrit (%)	41 ± 2	39.1 ± 0.35	40.03 ± 0.07	40.90 ± 0.95	37.1 - 63.5	40.67 ± 0.61	40.23 ± 0.57	43.10 ± 0.06	41.77 ± 0.70	38.8 - 68.7
Mcv (fl)	59.5 ± 1.0	60.9 ± 0.9	56.2 ± 0.6	57.3 ± 1.1	57.8 - 75.4	64.7 ± 1.2	64.3 ± 0.9	59.4 ± 1.0	59.8 ± 1.4	57 .5 - 76.6
Mch (pg)	20.7 ± 0.5	21.3 ± 0.3	19.9 ± 0.2	20.2 ± 0.5	17.8 - 25.1	21.6 ± 0.4	21.4 ± 0.5	20.0 ± 0.3	20.1 ± 0.4	16 .9 - 25.1
Mchc (pg)	34.7 ± 0.2	35.1 ± 0.1	35.3 ± 0.06	35.2 ± 0.2	26.5 - 37.9	33.5 ± 0.1	33.3 ± 0.4	33.7 ± 0.1	33.6 ± 0.2	2 6.8 - 37.7
Rdw (%)	12.7 ± 0.6	11.9 ± 0.3	11.1 ± 0.2	11.3 ± 0.3	13.1 - 16.9	13.0 ± 0.2	13.7 ± 0.06	12.1 ± 0.09	12.3 ± 0.3	14.2 - 18.0
Plt (x10^3 cells/µl)	949 ± 110	964 ± 88	784 ± 65	1131 ± 70	751 - 2390	80 7 ± 70	831 ± 46	857 ± 101	964 ± 24	771 - 2618
Mpv (fl)	8.5 ± 0.6	7.6 ± 0.2	8.8 ± 0.6	7.7 ± 0.3	5.8 - 9.6	8 .9 ± 0.4	8.6 ± 0.1	8.3 ± 0.2	7.9 ± 0.06	5.8 - 238.0

SUPPLEMENTARY VIDEO

Movie S1. 3D reconstruction of MR images after intracranial injection of Gd(III)-functionalized SNAs. Shown is a 360-degree 3D reconstruction of an MRI performed on the excised brain of a tumor-bearing mouse injected intracranially with Gd(III)-SNAs. The region in gray is the entire excised brain and the region in red is defined by the penetration of the Gd(III)-SNAs.